ISBN 978-93-84422-22-6
Proceedings of 2015 International Conference on Chemical, Mettalurgy and Environmental Engineering (CMAEE 2015)
Istanbul (Turkey), June 3-4, 2015 pp. 318-324

The Effect of Al‑8%B Master Alloy and Heat Treatment Conditions on the Microstructure and Mechanical Properties of an A518 Aluminium Alloy

A.Amerioon[1], Gh. Ashuri[2] and M. Emamy[3*]

[1]School of Metallurgy and Materials, College of Engineering, University of Tehran, Tehran, Iran

[2*]Corresponding author: Phone & Fax: (+98-21) 82084083, Email: emamy@ut.ac.ir

***Abstract*:** *In this research the effect of different amounts of Al–8%B grain refiner on the macro and microstructural features of A518 aluminium alloy were investigated. The optical microscopy, scanning electron microscopy equipped by EDX analyzer and X-ray diffraction analysis were used to investigate the microstructures and their phases. The results showed that B reduces the average grain size of the alloy. T6 heat treatment was applied for all specimens before tensile testing. It was also found that with the addition of 0.05%B, the ultimate tensile strength (UTS) and elongation values enhanced from 245 to 315.4 MPa and 8.36% to 10.1%, respectively. Significant improvements in UTS and elongation values were obtained after T6 heat treatment. Study of the fracture surfaces illustrated an inter-dendritic mode of fracture in unmodified alloy and the addition of Al–8B grain refiner changed the fracture behavior to ductile.*

Keywords: *Al–8B grain refiner, average grain size, UTS, inter-dendritic.*

1. Introduction

Aluminium-based alloys are widely used as aerospace and automotive components, because of their high specific strength, stiffness and formability. The Al-Mg alloys have attractive properties for applications where good combination of mechanical strength, elongation and thermal fatigue resistance is required [1]. A518 aluminium casting alloy is non-heat-treatable, has excellent corrosion resistance, machinability, high ductility, poor cast-ability, difficulties to polish and attain a uniform appearance after anodizing. It has poor weld-ability and braze-ability. This alloys are used for die cast marine fittings, ornamental hardware, ornamental automotive parts, and other applications requiring the highest corrosion resistance [2].

The Al-Mg binary phase diagram is shown in Figure. 1 (c). Temperatures which were experienced by the alloys in action for this range of Mg concentration, are well below the solvus line; Indicating that both α- and β-phases are present when the system is at equilibrium. That means Mg needs to diffuse out of the bulk and β-phase precipitates when the temperature is below 200-240 ^{0}C. These low to modest temperatures are readily experienced by the components of ships in service, which contributes to the susceptibility of IGC and SCC over the entire life of the ship [3, 4].

The effect of microstructural parameters such as the nature of precipitation on the matrix and size and distribution of grain boundary precipitates or grain size, play an important role in the mechanical properties of Aluminium alloys [5]. The grain size of the Al-Mg alloys tends to be rather large and grain refinement has been found to play a vital role in cast and wrought alloys. Grain refinement provides improved mechanical properties; it also improves the uniformity of structure throughout the casting, including a finer distribution of second phase and micro porosity [5-7].

http://dx.doi.org/10.17758/UR.U0615239

This investigation has been carried out to improve tensile properties of the A518 aluminium casting alloy by adding Al-8%B master alloy and applying heat treatment which are more economical and simple when compared to other methods such as rapid solidification and mechanical alloying

2. Experimental

The primary A518 alloy ingots were prepared by melting of pure Al (99.8%) and Mg (99.9%) in an electrical resistance furnace. After melting Al in a 10kg SiC crucible and heating up to 800 ^{0}C, Mg was added into the molten Al to prepare Al-8%Mg alloy. The chemical composition of Al-8%Mg alloy used in this study is shown in Table 1. Then, the primary ingots were cut into small pieces to fit in a small graphite crucible (1 kg capacity) and re-melted in another electrical resistance furnace. After stirring and cleaning off the dross, molten was poured into a cast iron mould which was preheated up to 220 ^{0}C. This mould was made according to the ASTM B108/B108M-12E1 standard (Fig. 1a). Tensile testing was carried out in a computer controlled tensile testing machine (SANTAM-STM20) at a constant cross-head speed of 1 mm/min. Microstructural studies were made on the polished sample surfaces which were selected from the gauge length portion of the test bars (with 6 mm diameter). Metallographic specimens were prepared through standard routines by polishing. In order to investigate the grain size of the refined samples, the samples were etched by Poultan's reagent (12ml HCl, 6ml HNO_3, 1mlHF, 1ml H_2O). Average grain size of the specimens was measured according to the ASTM E-12 standard, using an optical microscopy equipped with an image analysis system (ClemexVisionPro.Ver.3.5.025). Keller's reagent was also used for microstructural studies after polishing the cast specimens. The microstructures were characterized by an optical microscopy and a Cam Scan MV2300 scanning electron microscopy (SEM) which was equipped with EDX detector. The existing phase seen in the structure of A518 alloy were determined through X-ray diffraction (XRD) analysis using an XPert Philips (30 kV and 25mA) diffractometer with Cu Ka radiation (λ=1.5405˚A). As-cast specimens were solutionized at 440 ^{0}C for 9 h, quenched in water and artificially aged in 175 ^{0}C for 5 h (T6 heat treatment).

Table1- Chemical composition of Al-8%Mg Casting alloy.

Mg (wt. %)	*Si (wt. %)*	*Ni (wt. %)*	*Fe (wt. %)*	*Cu (wt. %)*	*Mn (wt. %)*	*Sn (wt. %)*	*Al (wt. %)*
7.5-8.5	**< 0.35**	**< 0.15**	**< 1.8**	**< 0.25**	**< 0.35**	**< 0.15**	**Base**

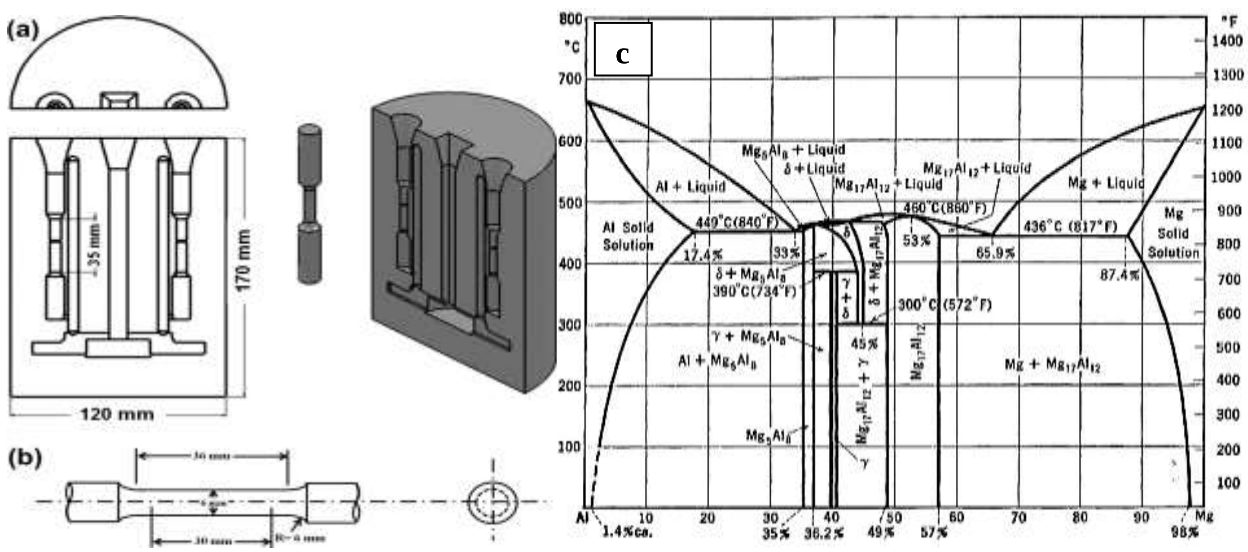

Fig. 1: (a) Cast iron mould (b) tensile samples dimensions. (c) Al-Mg binary phase diagrams [8].

3. Results and discussion

3-1 Microstructural characterization

The basic microstructure of the A518 aluminium alloy, shown in Fig. 2 (a) According to Al–Mg binary phase diagram, the microstructure of Al–8%Mg alloys contains primary α-Al (Mg) phase and eutectic structure;

In other words β-Al_3Mg_2 intermetallic and α-solid solution phase are formed. Fig. 2 (a), (b), (c) and (d) show the change in dendrite morphology of the A518 alloy after adding grain refiners. It is observed that grain refiner additions have significantly influence on DAS and causes decrease of it. The optical microstructures of B refined alloy revealed a rosette-like microstructure of primary α-Al grains solid solution surrounded by inter-dendritic secondary phases. From Fig. 2, it is noticeable that grain refinement enhances the number of grain boundaries and therefore promotes a more homogeneous distribution of intermetallic precipitates. The macrostructures of the A518 aluminium cast alloys before and after grain refinement by Al–8%B master alloy are shown in Fig. 3.

X-ray diffraction pattern was undertaken for phase identification of the refined alloy with 1 wt. % of B. The XRD analyses are shown in Fig. 4 (a). The XRD results clearly shows the presence of α-Al and Al_3Mg_2 and AlB_2 in the as cast alloy. Also as in the majority of aluminium alloys, impurities of iron and silicon can greatly contribute to the phase composition and properties of aluminium alloys. And the presence of iron or silicon impurities can result in the formation of such phases as Al_{15} (Fe, Mn)$_2Si_3$ and Mg_2Si, which possesses more favorable skeletal morphology [9]. The amount of this phase that is much low and X-ray diffraction pattern cannot show it. Fig. 4 (b) shows the effect of various amounts of Al–8%B grain refiner on the average grain diameter of the specimens. The study of refined specimens showed the presence of different macro and microstructural features, which may result in different mechanical properties. From Fig. 4 (b), the optimum amounts of B was determined to be 0.5 wt. %. For mechanisms of grain refining process in some study, the presence of some particle like AlB_2 is proposed to be effective for grain refinement. AlB_2 intermetallic phase is known to be a potential nucleating site for aluminium. It is resulted that the value of AlB_2 particles (which presented in the melt from the addition of Al–8%B master alloy type grain refiner) is much lower than those of grains [10, 11].

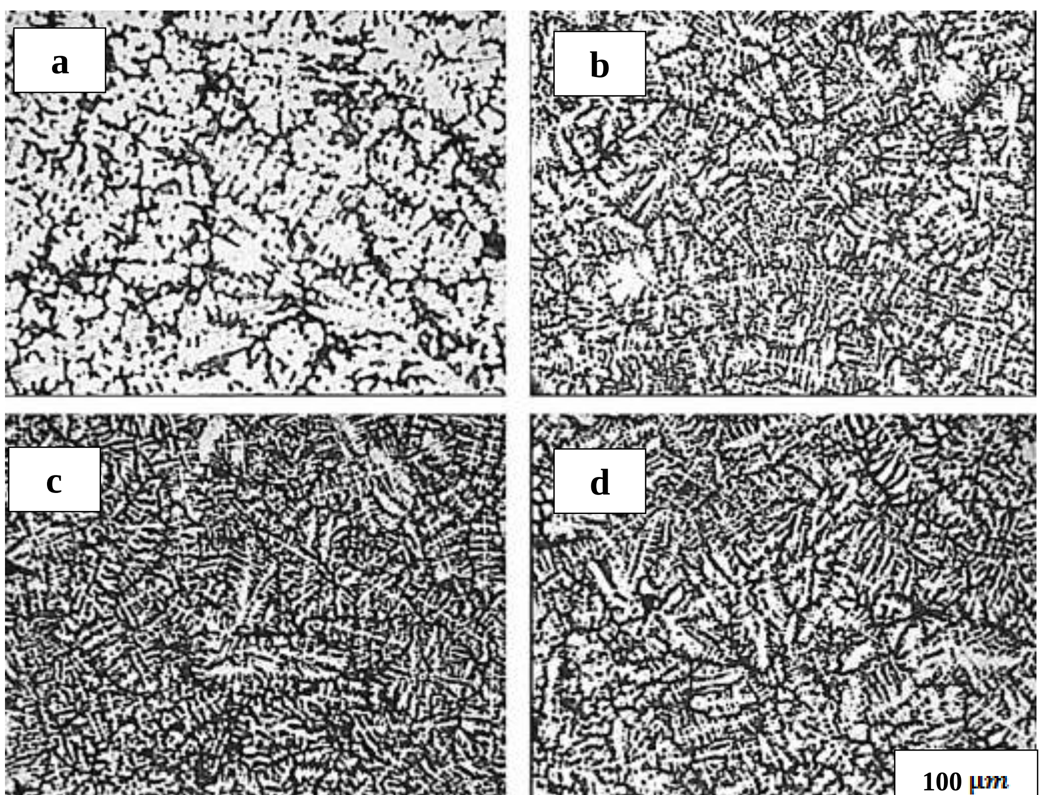

Fig. 2: (a) Microstructure of A518 alloy (b) A518+0.03%B (c) A518+0.1%B (d) A518+ 1% B.

http://dx.doi.org/10.17758/UR.U0615239

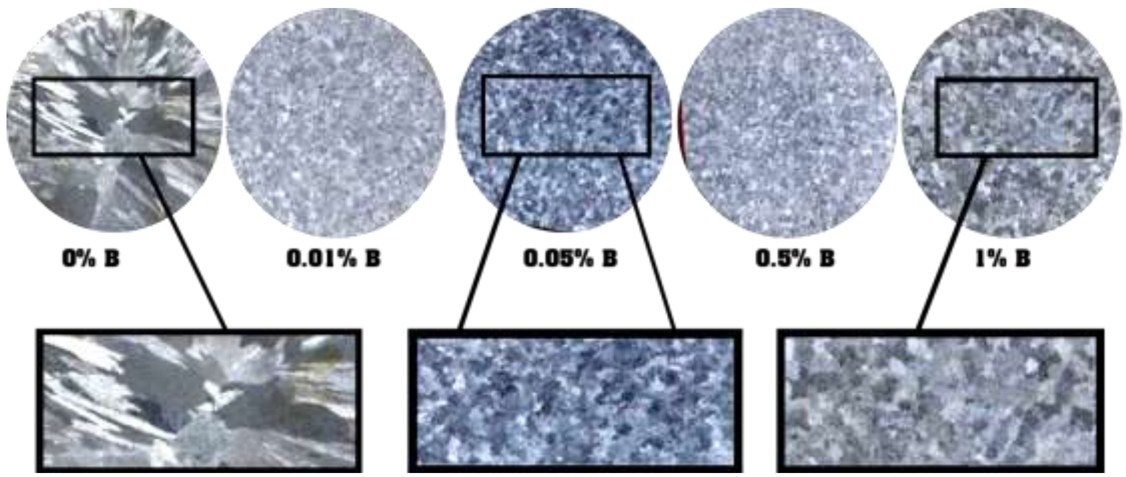

Fig. 3: Macrostructures of A518 alloy after grain refining by Al-8B master alloy.

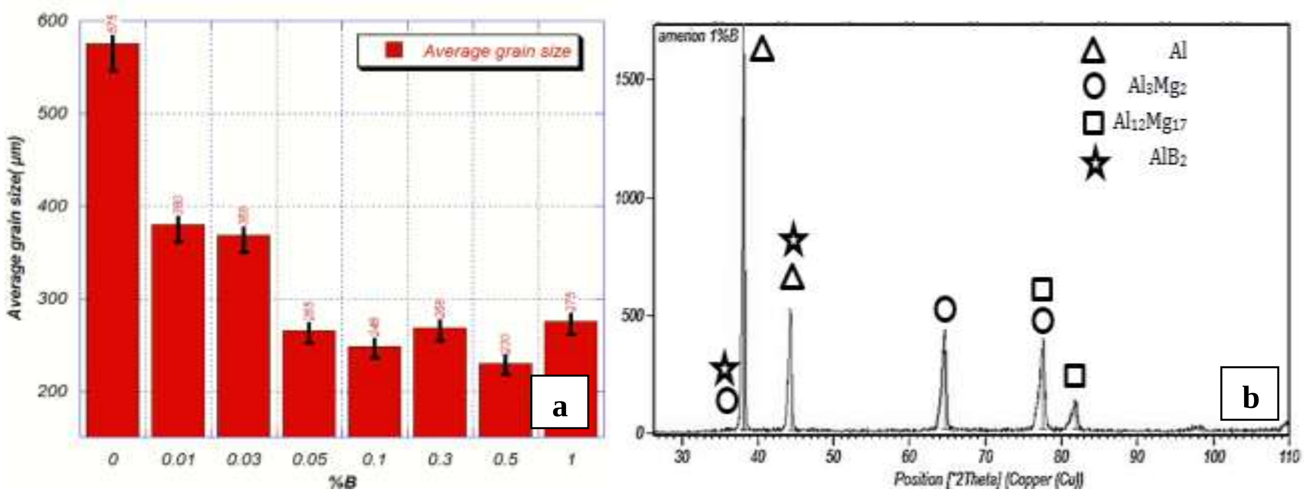

Fig. 4: (a) Grain size variations with B contents (b) X-ray diffraction patterns of 1.0% B-refined specimen.

3.2 Tensile properties

Fig. 5 illustrates the UTS and El % values of the as-cast A518 aluminium alloy with different amount of Al-8%B master alloy before and after heat treatment. This fig indicates that the addition of different amount of B enhances the UTS and elongation values results. The main reason for this improvement is high probably due to the reduced grain size of the alloy, and advantages of morphology and size of the α-Al primary phase and eutectic phases, as well as SDAS, which is leading to a finer distribution of intermetallic phases. It is well known that according to Hall–Petch theory: The finer the grains, the higher the strength [12].

To take advantage of the precipitation-hardening reaction, it is necessary first to produce a solid solution. After solution treatment and quenching, hardening is achieved either at room temperature (natural aging) or with a precipitation heat treatment (artificial aging). After solutionizing heat treatment, the intermetallic phase is solute in the matrix. Theory of dislocations can explained this increase in tensile strength after T6-treatment. In other words, obstructions to the motion of dislocations are happened by precipitated intermetallic particle that exist on the matrix after T6-treatment. Hence, increases of tensile strength can relate to such obstacles that postpone the motion of dislocations.

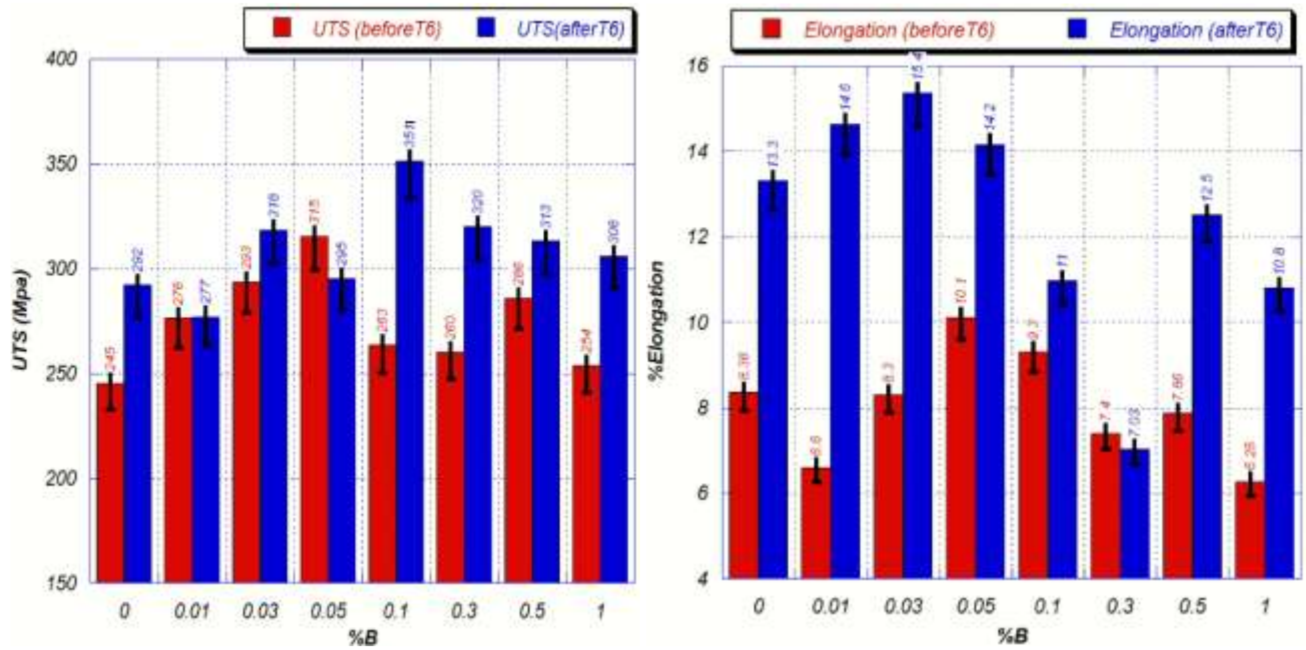

Fig. 5: UTS and elongation values of the A518 alloy samples as function of B content.

3.3. Fractography of tensile specimens

Fig. 6 illustrates the fracture surfaces of the un-modified alloy which represent inter-dendritic mode of fracture. As shown in Fig. 6, some shrinkage pores are observed on the fracture surface of A518 aluminium alloy. Shrinkage porosity resulting from incomplete feeding of α-Al dendrites during solidification that can create big void in the alloy structure. It is clear from Fig. 7 that grain refining by Al-8%B master alloy on A518 aluminium alloy causes the porosity content decreases when minor content of Al-8%B master alloy added. But in higher amount of refiner element, the porosity content increased significantly. The increase in porosity content with the addition of higher Al-8%B master alloy is high probably related to the formation of extensive number of nucleation sites during solidification, which can encourage the pasty mode of solidification [13]. There are some casting configurations, where the addition of extra grain refiner causes an increase in porosity content. This was clearly shown in a study by Easton and St. John, where an increase in the amount of refiner resulted in an increase in porosity content of the cast specimens. They found that although the amount of hot cracking decreases as the refiner level increases, the amount of localized porosity increases; because inter-dendritic feeding becomes more difficult during solidification [14]. Therefore, lower tensile properties of 1%B addition specimen of A518 aluminium alloy in comparison with other specimens that refined with Al-8%B master alloy can be due to the increased porosity at higher Al-8%B master alloy content.

Fig. 8 shows SEM images of fracture surfaces of 0.5%B addition specimen. Grain refining of the alloy and improving the morphology of α-Al phase, cause the domination of ductile mode of fracture. When stress is applied, the matrix plastically deformed, gradually transferring stress to the intermetallic particles. The behavior of the intermetallic particle depends on the relative strength of the interface and the matrix. When the interface is strong enough, the load is transferred to this particles and fracture occurs as soon as the threshold stress is reached.

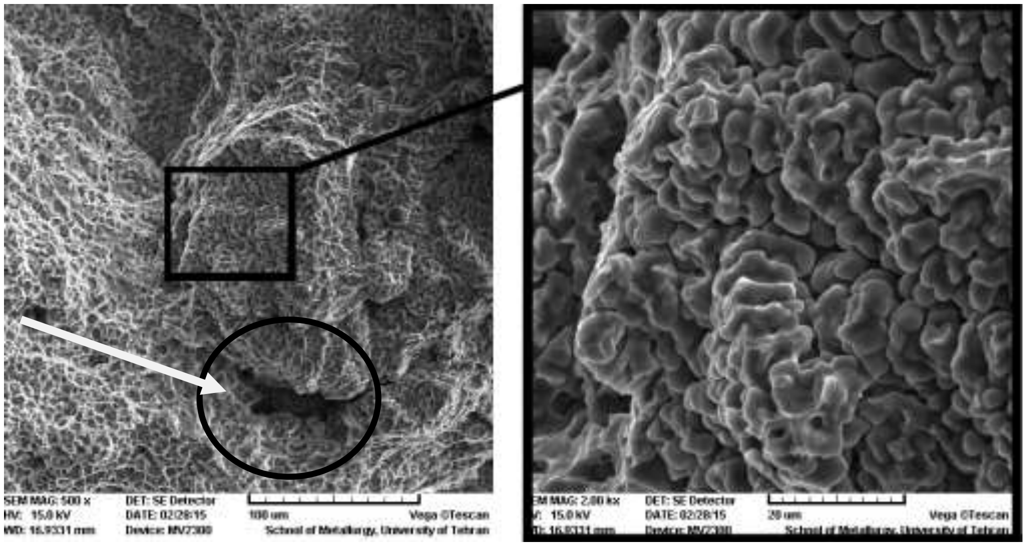

Fig. 6: SEM micrograph of fractured surface of A518 alloy.

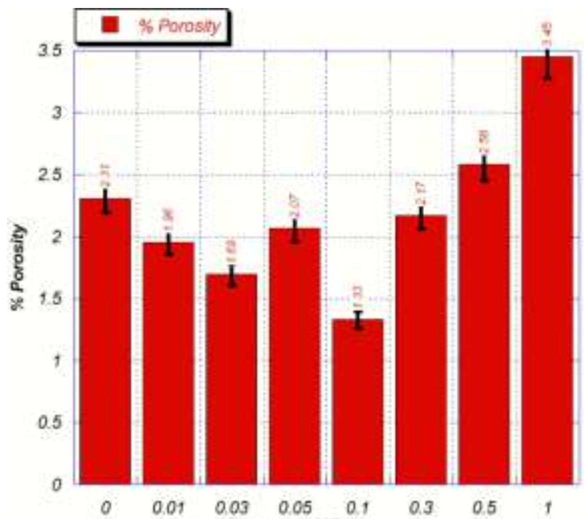

Fig. 7: The porosity percentage of samples with different amounts of Al-8%B master alloy.

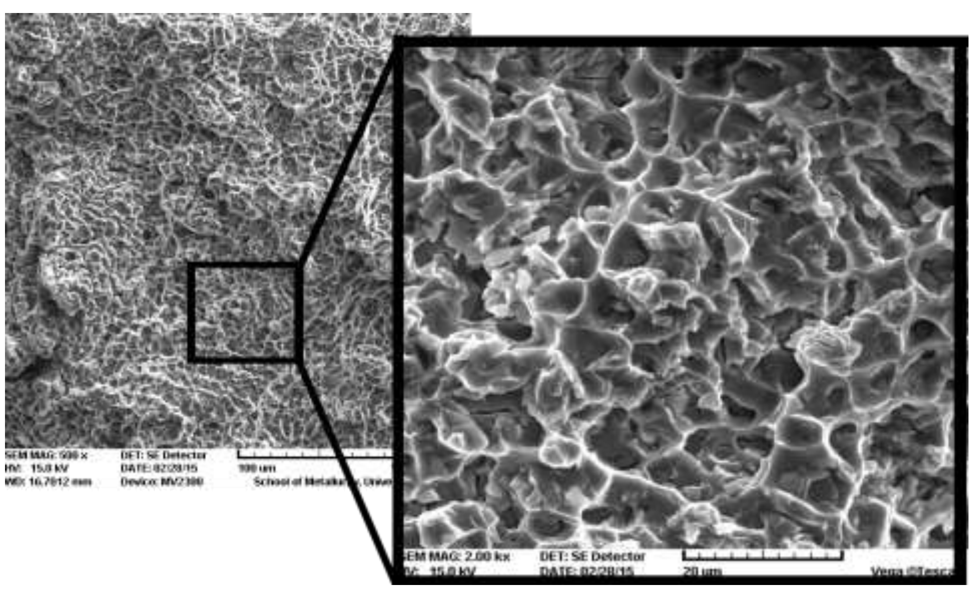

Fig. 8: SEM micrograph of fractured surface of A518 aluminium alloy with 0.5%B addition.

4. Conclusions

In current research the effects of different amount of Al-8%B master alloy were investigated on the microstructure and tensile properties of A518 Al-Mg alloy. The following conclusions can be drawn:

1) The addition of Al-8%B master alloy greatly reduced the grain size of A518 alloy.

2) The addition of Al-8%B master alloy significantly improved the mechanical properties of A518 alloy owing to the improvement in microstructure.

3) Fractography examination of the fracture surfaces of the refined alloy shows more ductile fracture by Al-8%B master alloy addition.

5. Acknowledgements

The authors would like to thank University of Tehran for financial support of this research.

6. References

[1] L. F. Mondolfo, "Aluminium Alloys Structure and Properties", London, Butterworth, 1976.

[2] *Properties and Selection Nonferrous Alloys and Special-Purpose Materials*. Ohio: ASM; 1992, Vol. 2, pp. 653-654.

[3] L.I. Kaigorodova: *The Physics of Metals and Metallography,* 1994, vol. 78, pp. 490-96.

[4] A.J. Davenport: *Aluminium Alloys, Pts 1 and 2 - Research through Innovation and Technology,* 2006, pp. 641-46.

[5] D. Hamana, S. Nebti, S. Hamamda, "Effect of the Zirconium Addition on the Microstructure of Al + 8 WT% Mg Alloy", J Scripta Metall. Mater. 24 (1990) 2059-2064.
http://dx.doi.org/10.1016/0956-716X(90)90486-Z

[6] D. G. Mccartney, "Grain Refining of Aluminium and Its Alloys Using Inoculants", Int. J Mater. Rev. 34 (1989) 247-260.
http://dx.doi.org/10.1179/imr.1989.34.1.247

[7] P. S. Mohanty, J. E. Gruzleski, "Mechanism of Grain Refinement in Aluminium", J Acta Metall. Mater. 43 (1995) 2001-2012.
http://dx.doi.org/10.1016/0956-7151(94)00405-7

[8] L. F Mondolfo, "Metallography of Aluminium Alloys, Prentice- JOHN WILEY & SONS, INC. NEW YORK, (1943).

[9] V.S. Zolotorevsky, N.A. Belov, M.V. Glazoff, Casting Aluminium Alloys, vol. I, UK, 2007, Pp .386-396.

[10] Seyed Ebrahimi SH, Emamy M. Effects of Al–5Ti–1B and Al–5Zr master alloys on the structure, hardness and tensile properties of a highly alloyed aluminium alloy. Int Mater Rev Mater Des 2010; 31: 200–9.

[11] Murty BS, Kori SA, Chakraborty M. Grain refinement of aluminium and its alloys by heterogeneous nucleation and alloying. Int Mater Rev 2002; 47: 3–29.
http://dx.doi.org/10.1179/095066001225001049

[12] Hertzberg RW. *Deformation and fracture mechanics of engineering materials*. 4th ed. John Wiley & Sons Publication, Inc.; 1996.

[13] Easton MA, St John D. Grain refinement of aluminium alloys: Part II. Int J Mater Res Adv Technol 1996; 87: 216–20.

[14] Easton MA, St John DH. The effect of grain refinement on the formation of casting defects in alloy 356 castings. Int J Cast Met Res 2000; 12: 393–408.